
Article:
Zhang, Huifa, Clark, James H. orcid.org/0000-0002-5860-2480, Geng, Tong et al. (2 more authors) (2020) A Carbon Catalyst Co-Doped with P and N for Efficient and Selective Oxidation of 5-Hydroxymethylfurfural into 2,5-Diformylfuran. ChemSusChem. pp. 1-12. ISSN: 1864-564X

https://doi.org/10.1002/cssc.202001525

FULL PAPER

A carbon catalyst co-doped with P and N for efficient and selective oxidation of 5-hydroxymethylfurfural into 2,5-diformylfuran

Huifa Zhang,[a] James H. Clark,[b] Tong Geng,[a] Huixian Zhang,[c] and Fahai Cao*[a]

[a] Huifa Zhang, Dr.Tong Geng, Prof. Fahai Cao
Engineering Research Centre of Large Scale Reactor Engineering and Technology of Ministry of Education, East China University of Science and Technology, Shanghai 200237, China.
E-mail: fhcao@ecust.edu.cn
[b] Prof. James H. Clark
Green Chemistry Centre of Excellence, University of York, York YO105DD, UK.
E-mail: james.clark@york.ac.uk
[c] Huixian Zhang
SINOPEC North China E&P Company, Zhengzhou 450006, China.
E-mail: zhanghuixian.hbsj@sinopec.com

Supporting information for this article is given via a link at the end of the document.

Abstract: A novel designer N and P co-doped carbon material has been developed to catalyze the conversion of 5-hydroxymethylfurfural (HMF) to 2,5-furandialdehyde (DFF) with unprecedented yield and selectivity and demonstrating a synergistic effect between the heteroatoms. The desired catalyst was first synthesized via a pyrolysis method using urea as the nitrogen and carbon source followed by calcination with phytic acid solution as the phosphorus source. The mass ratio of phytic acid to C_3N_4, and calcination temperature were varied to investigate their effects on catalysts synthesis and microstructure as well as subsequent catalytic activity in simple reaction systems under oxygen. The effect of reaction conditions on the final HMF conversion and DFF selectivity were also investigated systematically. The P-C-N-5-800 catalyst obtained with the optimized annealing temperature of 800 °C and mass ratio of phytic acid/C_3N_4 of 5, enabled a 99.5% DFF yield at 120 °C for 9 h under 10 bar oxygen pressure, being the highest among any reported metal-free heterogeneous catalyst to date. The excellent performance of P-C-N-5-800 could be ascribed to the synergistic function of N and P heteroatoms, as well as its high content of the graphitic-N and the P-C species within the carbon structure. Reusability studies shows that the P-C-N-5-800 catalyst was stable and re-usable without deactivation. These results strongly suggest that P-C-N-5-800 is a promising catalyst for large-scale production of DFF in a green manner.

Introduction

The chemical industry is accelerating the depletion of traditional fossil reserves and bringing increasing pressure on environmental issues, encouraging the greater use of clean and renewable resources. Biomass, the only practical and sustainable source of carbon for chemicals, has drawn great attention from researchers. HMF has been identified as one of the top 10 biomass-derived renewable platform chemicals. [1] HMF is primarily obtained from biomass by dehydration of C6 saccharide or cellulose.

The molecule 5-hydroxymethylfurfural (HMF) possesses a hydroxyl group and an aldehyde group at the 2,5 positions of the furan ring, which enable it to perform different types of reactions, such as hydrogenation,[2-3] oxidation,[4-5] rearrangement,[6] decomposition[7] and polymerization,[8] et al. HMF can be converted to value-added fine chemicals and liquid fuels, such as levulinic acid,[7] 2,5-furandialdehyde (DFF),[9-10] 2,5-furandicarboxylic acid (FDCA).[11-12] Among them, DFF is one of more attractive products. DFF contains two peculiar symmetrical reactive aldehyde groups on its furan ring, which make it suitable for a wide range of important applications via transformation to other high value-added chemicals including monomer, fuels and additives. DFF is mainly prepared by selective oxidation of the hydroxyl group of HMF to an aldehyde group, as shown in Scheme 1.

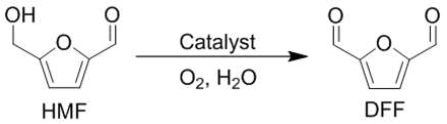

Scheme 1. Oxidation of HMF to DFF

The challenge of the above oxidation, however, lies in the development of suitable catalysts. Homogeneous catalysts, such as metal nitrate,[13] metal nitrite[14] and NaBr,[15] generally lead high DFF yields under mild reaction conditions, but are associated with equipment corrosion and separation difficulties. Heterogeneous catalysts including noble or transition metal catalysts and metal-free carbon-based catalysts have also been extensively studied for this reaction. Noble metals, such as Rh,[16] Au,[17], Ru[17] and Pt[18] can enable high activity as well as high selectivity for producing DFF from HMF, but their cost and scarcity restricts large-scale commercial production using them. Non-precious metal catalysts such as those based on manganese,[19-21] vanadium[22-25] and cobalt,[26] always suff from the problems of leaching, poor stability and high cost as well as contamination of the products. Therefore, design of highly efficient and inexpensive metal-free heterogeneous catalysts for converting HMF to DFF is a high priority for future biorefineries and chemical manufacturing. There have been a few reports of the catalytic conversion of HMF to DFF using molecular oxygen over metal-free N-doped carbon catalysts. The first pioneering work was reported by Rathod in 2017 who showed that a free acid-base (CC-SO_3H-NH_2) catalyst could be used for catalyzing HMF, fructose, and glucose to

DFF.[10] The as-prepared catalyst contained −SO_3H and −COOH acidic di-functional groups and siloxypropylamine basic functional groups. High selectivity towards the conversion of HMF, fructose, or glucose to DFF was then demonstrated. The highest yield of 87% of DFF from HMF was obtained over CC-SO_3H-NH_2 catalyst at 140 °C for 9 h in dimethyl sulfoxide (DMSO) under a constant flow of O_2. Although the presence of acid in the catalyst could catalyze the hydrolysis of sugars to HMF, it also catalyzed the polymerization or degradation of HMF, resulting in a decrease in DFF yield. Later, NC-950, one kind of nitrogen-doped carbon catalyst, was developed by Zhang et al. for converting HMF to DFF using HNO_3.[27] A 95.1% yield of DFF was achieved, while HMF was completely transformed at 10 bar oxygen pressure at 100 °C for 14 h in the presence of catalytic HNO_3. However, the addition of HNO_3 rendered the above reaction out of the scope of green chemistry, and a long reaction time was required to ensure a good DFF yield.

Despite their promise, the achieved performances as well as the use of HNO_3 were far from satisfactory and the need for a smart metal-free catalyst is critical. C_3N_4 has recently received special attention due to its excellent electrocatalytic activity,[28] fascinating photocatalytic performance[29] and high stable thermal and chemical stability.[30] C_3N_4 has been used as a photocatalyst in selective oxidation of HMF to DFF with a 50 % of selectivity under real outdoor illumination.[31] Moreover, among the doped-carbon catalysts, N-doped carbons demonstrated astonishing activities owning to the high electronegativity of N atoms.[32] Carbon materials doped with N atoms have been widely employed in oxygen reduction reaction (ORR),[33-34] oxygen evolution reaction (OER)[35] and aerobic oxidation reactions.[36] Based on this, C_3N_4 was used as a nitrogen doped carbon oxidation catalyst for the direct oxidation of HMF to DFF.

Heteroatoms co-doping is an efficient strategy to improve the catalytic performance of carbon catalysts owing to the synergistic effect between the dopants. On the other hand, the lower electronegativity of P element renders P partially positively charged in the P doped carbon materials, the opposite to that of the N atoms in the N doped carbon materials, and in spite of the fact that P and N have the same number of valence electrons. It has been reported that P can promote the carbonization of N-doped carbon during the heat treatment, resulting an improvement on the electrical conductivity of N-doped carbon materials.[37] It is hypothesized in this work that a design based on a heteroatom co-doped carbon material using nitrogen and phosphorus might create a synergistic effect between N and P for the conversion of HMF to DFF.

In the current work, a nitrogen and phosphorus heteroatom co-doped carbon material was designed and synthesized via a pyrolysis method using urea as a nitrogen and carbon source followed by calcination with phytic acid solution as a phosphorus source. Catalytic performance measurements were carried out in a 70 ml Teflon-lined stainless-steel autoclave for selective aerobic oxidation of HMF to DFF without adding any other chemicals. The mass ratio of phytic acid to C_3N_4 and the calcination temperature were varied to investigate their effects on the catalyst synthesis and subsequent catalytic activity and DFF selectivity. The catalyzed reactions were performed systematically to give an optimized solution. Detailed characterization of the catalysts was also carried out to unravel the underlying mechanism of catalysis function. Obviously, such an eco-friendly and robust metal-free catalyst might pave the way for large-scale production of bio-based from HMF to DFF from HMF.

Results and Discussion

Characterization of carbon catalysts

The synthesis process for P-C-N is illustrated in Scheme 2. Firstly, a Nitrogen-doped carbon material C_3N_4 was prepared via a pyrolysis method using urea as a nitrogen and carbon source (Scheme 2). Phytic acid solution as a phosphorus source was introduced to the obtained C_3N_4 with different mass ratios to obtain a series of P-C-N-n-T materials.

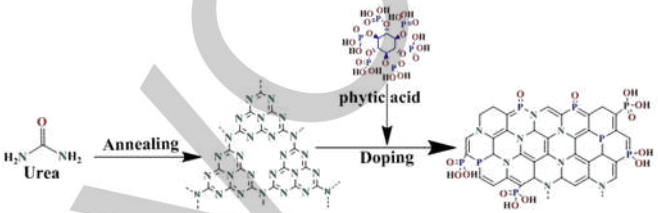

Scheme 2. Synthesis process of P-C-N catalysts

The synthesized P-C-N carbon samples have anomalous surface morphologies as shown by SEM images (Figure 1 (a, b, c, d) and Figure S1. (a, b, c, d)). It is obvious that the morphology of the P-C-N catalysts was greatly affected by the annealing temperature and the mass ratio of phytic acid/C_3N_4. TEM images of the as-synthesized carbon catalysts show that the number of pores of the materials is increased as expected with increasing pyrolysis temperature (Figure 1). High resolution TEM images of the P-C-N-5-800 (Figure 2), reveal abundant irregular micropores. BET results further confirmed the above observation that the average pore size was mainly distributed at around 1.2 nm. In addition, the above results further indicate that the size of pores in the catalyst has a negative correlation with the mass ratio of phytic acid/C_3N_4 (Figure S1). The micropores in the P-C-N catalysts will assist the mass diffusion of reactants and products, and thereby guarantee sufficient adsorption sites for both reactants and products. Moreover, N and P atoms are successfully incorporated into the carbon framework with a homogeneous distribution as shown by the STEM-EDS elemental mapping images of P-C-N-5-800 (Figure 2).

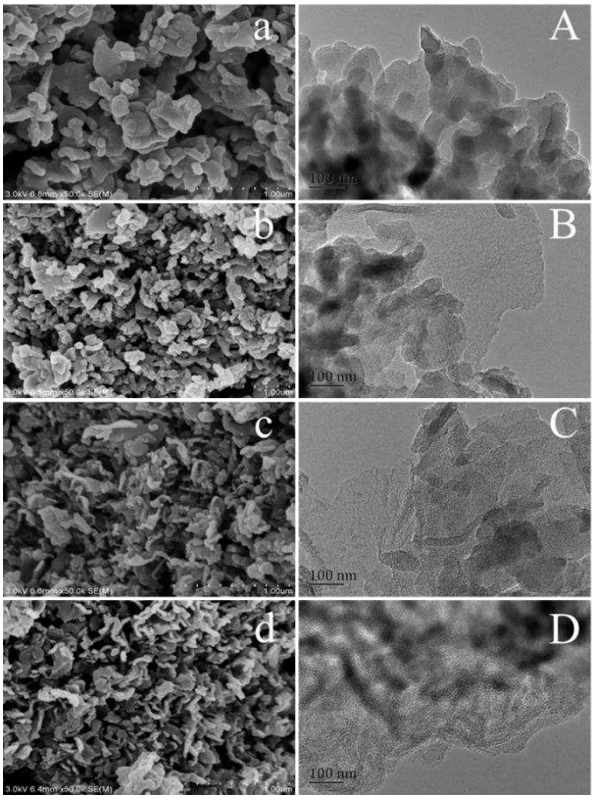

Figure 1. SEM (a, b, c, d) and TEM (A, B, C, D) images of P-C-N-5-T carbon samples synthesized with different annealing temperature, a and A corresponding to P-C-N-5-600, b and B corresponding to P-C-N-5-700, c and C corresponding to P-C-N-5-800, d and D corresponding to P-C-N-5-900.

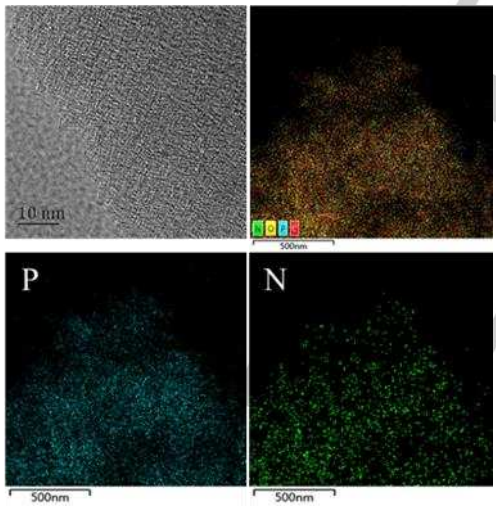

Figure 2. High TEM image of the P-C-N-5-800 catalyst and elemental mapping of the P-C-N-5-800 catalyst.

XRD patterns of the P-C-N-5-T material are shown in Figure 3. It is evident that all four carbon samples display two broad peaks at around 24 degrees and 44 degrees, indicating their graphite-like structures with a (002) and a (101) reflections, respectively. In addition, the presence of the broad XRD reflections indicate that the microstructures of the as-synthesized carbon materials are highly disordered as shown by TEM results. The intensity of peaks at around 44 degree of P-C-N-5-T increased with increasing annealing temperature. However, the results from the study of the P-C-N-n-800 series demonstrated the opposite phenomenon, whereby the peaks at 44 degrees decrease with increasing mass ratio of phytic acid/ C_3N_4 (Figure S2). The variation in intensity of the peaks on the XRD patterns indicates that the annealing temperature and the mass ratio of phytic acid/ C_3N_4 have a great influence on the structure of the catalysts.

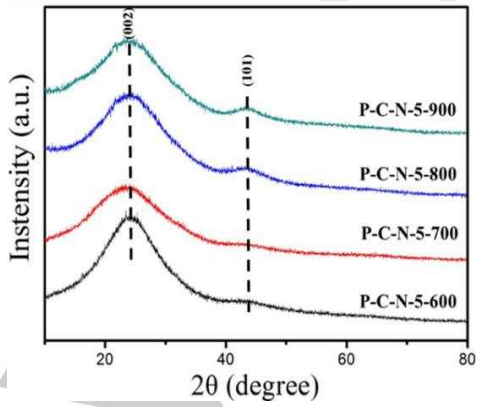

Figure 3. XRD patterns of the prepared P-C-N-5-T carbon samples synthesized with different annealing temperature.

Raman spectra of the P-C-N-5-T carbon samples are shown in Figure 4. Typical features of disordered or nanocrystalline graphitic carbon can be seen from these images.[38] All the samples exhibit two obvious peaks at about 1360 cm^{-1} and 1580 cm^{-1}. The former peak at 1360 cm^{-1} is attributed to D-band, while the latter corresponds to G-band. The D-band in graphitic materials is often referred to the disorder band or the defect band, and the G-band is evidence of a graphitized structure, as also shown above by XRD results. The I_D/I_G of P-C-N-5-600, P-C-N-5-700, P-C-N-5-800, and P-C-N-5-900 is 1.51, 1.54, 1.59 and 1.62, respectively, while the I_D/I_G is 1.49, 1.53, 1.59 and 1.70 for P-C-N-2.5-800, P-C-N-4-800, P-C-N-5-800, and P-C-N-7.5-800 respectively. It is interesting that the intensity ratio of I_D/I_G of the as-prepared carbon materials gradually increase with increasing mass ratio of phytic acid/C_3N_4 for the synthesis (Figure S3) as well as increasing annealing temperature (Figure 4). The increase in I_D/I_G of the P-C-N-5-T catalysts in Figure 4, together with the above TEM analysis, suggest that more defects instead of graphitization evolved in carbon structures under the high pyrolysis temperature, which reveal that the pyrolysis is a complicate process. On one hand, high pyrolysis temperature may favor the graphitization evolved in carbon structures, thus resulting in a decrease in I_D/I_G. On the other hand, more heteroatoms including N and P grafted on the carbon lattice had been peeled off from the carbon lattice under high pyrolysis temperature thus resulting in a higher percent defects in the as-synthesized carbon framework. This is consistent with the literature ever reported.[27,39-41] The increase in I_D/I_G of the P-C-N-n-800 catalysts can be attributed to the enhancement of phosphorous content, its size, and its preference for an sp3 configuration. The intensity ratio of D-band to G-band (I_D/I_G) is often used to investigate the defects in carbon materials induced by heteroatom doping, while defect sites are often the active sites of catalysts.[40] Therefore, improving the I_D/I_G of carbon samples can be expected to improve the activity of catalysts.

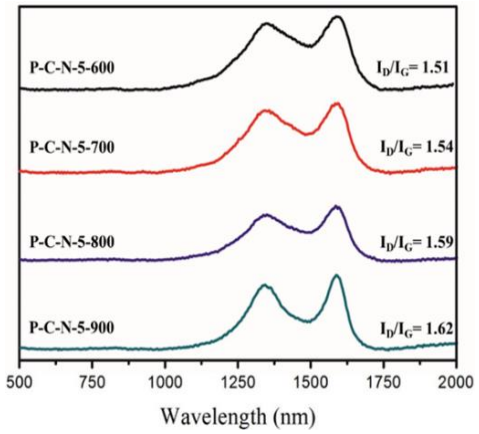

Figure 4. Raman spectra of the P-C-N-5-T carbon samples synthesized with different annealing temperature.

It is well known that the surface area of catalyst can play a significant role in heterogeneous catalytic reactions. Therefore, it is necessary to investigate the surface area of the carbon catalysts. N_2 adsorption-desorption isotherms of the carbon catalysts are depicted in Figure 5 and Figure S4. The isotherms of all carbon samples are typical type-I isotherms of which the adsorption capacity increased rapidly under low relative pressures, suggesting that the pores in the catalysts are mainly micropores. The H3 and H4 type hysteresis loops are observed at high relative pressures, suggesting that the carbon catalysts possess irregular structure, like those reported in the literature.[42] The surface area and the pore volume calculated by BET and DFT respectively are summarized in Table 1 and Table S1. The surface area of the carbon samples increased from 24.91 to1426.41 m²/g when the anneal temperature increased from 600 to 900 °C with especially large increases above 700 °C, whereas the surface area of the carbon samples decreased from 866.86 to 373.73 m²/g as a function of the increase in the mass ratio of phytic acid/C_3N_4 from 2.5 to 7.5. The pore volume of P-C-N-5-600, P-C-N-5-700, P-C-N-5-800, P-C-N-5-900 is 0.18, 0.17, 0.8, 1.31 cm³/g, while the pore volume of P-C-N-2.5-800, P-C-N-4-800, P-C-N-5-800, P-C-N-7.5-800 is 0.80, 0.76, 0.65, 0.32 cm³/g, respectively. The pore size of the carbon samples is mainly distributed at around 1.2 nm, suggesting that all samples have microporous character. The pore volume of these samples followed a similar trend with the surface area. Hence, the higher the annealing temperature, the greater the porosity.

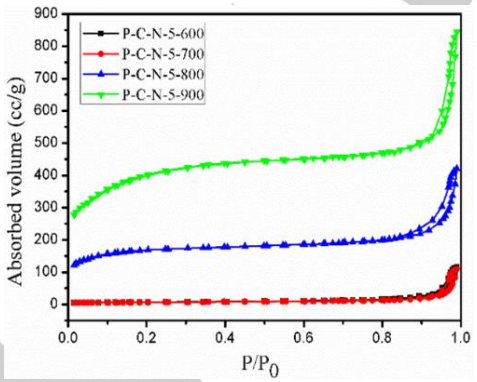

Figure 5. N_2 adsorption-desorption isotherms of P-C-N-5-T carbon samples synthesized with different annealing temperature.

Table 1. Physicochemical properties of P-C-N-5-T carbon samples synthesized under different annealing temperature.

Entry	Catalysts	BET Surface Area (m²/g)	Pore Volume (cm³/g)	Pore size (nm)
1	P-C-N-5-600	24.91	0.18	1.04
2	P-C-N-5-700	27.38	0.17	1.20
3	P-C-N-5-800	596.98	0.80	1.26
4	P-C-N-5-900	1426.41	1.31	1.20

XPS was used to investigate the nature of the N and P sites in particular (Figure 6). Predominant peaks occur at 284.6 eV, 532 eV, 400 eV, and 133 eV for the P-C-N-5-T carbon materials, corresponding to C, O, N, and P respectively. The successful incorporation of N and P into the carbon framework is clear and consistent with previous EDS mapping results (Fig 2). In each spectrum, the N 1s (Figure 7(a)) peak could be deconvoluted into three sub-peaks, at around 398.2 eV, 399.8 eV and 401.1 eV, corresponding to pyridinic-N, pyrrolic-N and graphitic-N, respectively.[43-46] The P 2p (Figure 7(b)) peak could be fitted into three sub-peaks, assigning to P-C (132.5 eV), P-N (133.4 eV) and P-O (134.2 eV) bonds accordingly.[40,47-48] The relative amounts of C, N, P and O in the P-C-N-n-T carbon samples calculated from XPS spectra are summarized in Table S2. The relative contents of N, P and O of the P-C-N-5-T carbon catalysts decreased with an increase in the annealing temperature. A positive correlation exists between the mass ratio of phytic acid/C_3N_4 and the relative contents of P and O in the P-C-N-n-800 carbon samples, while the relative contents of N exhibited an opposite trend. The relative ratios and the absolute ratios of the various species of N and P were summarized in Table S3 and Table S4, respectively. As could be observed, the relative ratios and the absolute ratios of graphitic-N and P-C gradually increase with an increase in pyrolysis temperature before 800 °C. Further increasing the pyrolysis temperature above 800 °C to 900 °C would result in a decrease in the absolute ratio of graphitic-N and P-C. The peak centered at 132.5 eV assigned to P-C was not observed in the spectrum of P-C-N-5-600, suggesting that P atoms were not incorporated into the carbon lattice at the annealing temperature of 600 °C. It was noteworthy that the graphitic-N content and the P-C content of the P-C-N-5-800 carbon catalysts reached a maximum at around 800 °C.

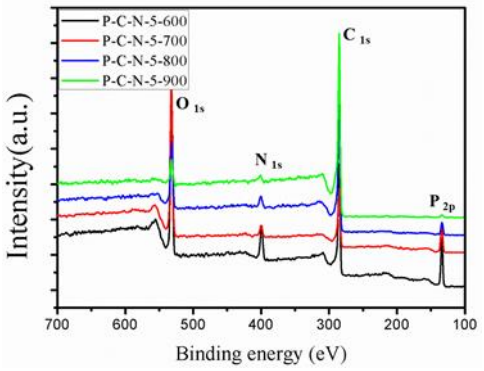

Figure 6. XPS scan spectra of P-C-N-5-T carbon samples synthesized under different annealing temperature.

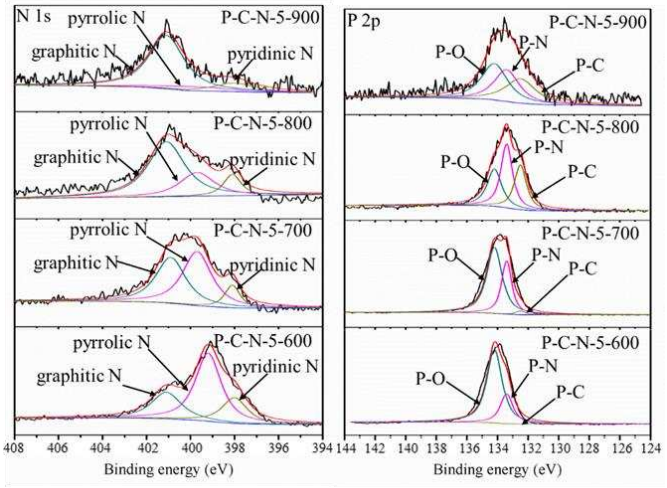

Figure 7. (a) XPS N1s spectra of P-C-N-5-T carbon samples synthesized under different annealing temperature; (b) XPS P2p spectra of P-C-N-5-T carbon samples synthesized under different annealing temperature.

Catalytic performance

Effect of the mass ratio of phytic acid/C_3N_4 in the process of catalyst synthesis on the catalytic aerobic oxidation of HMF to DFF

The performance of various carbon catalysts was studied using a 70 ml Teflon-lined stainless steel autoclave. The catalytic performance of the carbon catalysts was first investigated in MeCN at 120 °C and 10 bar O_2 pressure for 8 h. The results are summarized in Table 2. C_3N_4 and P-C-800 were also subjected to the same evaluation for comparison. C_3N_4 exhibits excellent catalytic activity (96.2% conversion) but poor selectivity (18.8% selectivity of DFF) under the given conditions. The P-C-800 catalyst, carbon doped with P atoms alone, shows good selectivity (100%) to DFF, but a relatively low conversion of HMF (31%). When P-C-N-2.5-800 was used, the conversion of HMF increased to 58.8%, and DFF selectivity increased to 96%. When the phytic acid/C_3N_4 mass ratio increased from 2.5 to 5, the conversion of HMF further increased to 93.6% and DFF selectivity increased to 100%. However, further increasing the mass ratio of phytic acid/C_3N_4 from 5 to 7.5 resulted in a dramatic decrease in DFF yield to 42.3%. The absolute content of graphitic-N of the P-C-N-n-800 catalysts studied by XPS characterizations first increased and then decreased (Table S4) with the increase of mass ratio of phytic acid/C_3N_4. There is a positive correlation between the graphitic-N concentration and HMF conversion. Thus, it is believed that the catalytic activity is related to the graphitic-N concentration in the catalysts which is in agreement with earlier reports.[27,41,49-50] These results suggested that the mass ratio of phytic acid/C_3N_4 played a pivotal role in determining the catalytic performance of the nitrogen and phosphorus co-doped carbon catalysts. It is worth noting that P-C-N-5-800 possesses the highest content of graphitic-N and P-C species but a lower surface area relative to P-C-N-2.5-800 and P-C-N-4-800. The graphitic-N and the P-C species content might be more important in the catalytic aerobic oxidation of HMF to produce DFF with molecular oxygen than is the surface area.

An extra control experiment was also performed by using a mixture sample of P-C-800 and C_3N_4 with mass ratio of 5 under the same oxidation conditions (Table 2). A lower yield of DFF (32.4%) was obtained from the mixed catalysts, with a 39.3% conversion of HMF and 82.4% selectivity to DFF. These observations indicated that there might be a synergistic effect between N and P in the co-doped carbon catalysts. Therefore, further investigation of the catalytic performance of carbon catalysts on the oxidation of HMF to DFF focused on the carbon catalyst obtained with the mass ratio of phytic acid/C_3N_4 of 5/1 (P-C-N-5-800).

Table 2. Oxidation of HMF to DFF over different carbon catalysts[a]

Entry	Catalyst	HMF Con. (%)	DFF yield (%)	DFF Sel. (%)
1	C_3N_4	96.2	18.1	18.8
2	P-C-800	31.0	31.0	100.0
3	P-C-N-2.5-800	58.8	56.4	96.0
4	P-C-N-4-800	77.7	77.7	100.0
5	P-C-N-5-800	93.6	93.6	100.0
6	P-C-N-7.5-800	42.7	42.3	99.0
7[b]	P-C-800 + C_3N_4	39.3	32.4	82.4

[a] Reaction conditions: HMF 1 mmol, catalyst 80 mg, 120 °C, MeCN 20 g, O_2 10 bar, duration 8 h.

[b] Catalyst: 13.4 mg C_3N_4 and 66.6 mg P-C-800.

Effect of the catalyst annealing temperature on the catalytic aerobic oxidation of HMF to DFF

As demonstrated, high annealing temperature could result in high surface area, which should facilitate the mass transfer of both reactants and products. However, it was also shown that the graphitic-N and P-C species contents might be more important in catalytic aerobic oxidation of HMF to produce DFF with molecular oxygen than the surface area. Further experiments were carried out to verify the effect of annealing temperature (600 - 900 °C) on the catalysis performance of the P-C-N-5-T catalyst with the fixed optimum phytic acid/C_3N_4 of 5/1. The results were depicted in Table 3. HMF conversion increased from 61.9% to 93.6% when the annealing temperature increased from 600 °C to 800°C, while the selectivity of DFF increased from 60.6 to 100%. However, with further increase in the annealing temperature, the conversion of HMF significantly decreased. These results are contrary to the results observed in the Table 2. HMF conversion over P-C-N-5-900 catalyst was lower than the conversion over other P-C-N-5-T catalysts in spite of higher graphitic-N contents it possessed. This might be ascribed to the fact that lower pyrolysis temperature facilitated the formation of the P-O species which has been proved closely associating with the catalytic activity of P doped carbon catalysts in oxidation reaction.[40,51] To confirm this point, the aerobic oxidation of HMF was conducted over the P-C-700 catalyst pretreated by annealing the phytic acid solution at 700 °C. The catalytic studies show that the aerobic oxidation of HMF over P-C-700 exhibited a higher conversion (48.8%) of HMF than the reaction over the P-C-800 catalyst (Table S6). XPS studies reveal that the P-C-700 has a higher content of P-O species and a lower content of P-C species than the P-C-800 catalyst (Table S5). Combination of the reaction results with the XPS characterizations suggest that the content of P-O species is closely associating with the catalytic activity of P doped carbon catalysts in oxidation reaction. Compared with the results in Table 3 and Table 2, it should be note that almost no difference on the selectivity of DFF was observed over P-C-N-n-800 catalysts, while the selectivity of DFF over P-C-N-5-T catalysts increased with the annealing temperature. This further confirms that the P-

C species of P doped carbon catalysts might be more conducive to the selectivity of DFF. These results together with the results in the Table 2 demonstrate that both the content of graphitic-N and P-O species of the P-C-N-n-T catalysts are crucial for the catalytic activity in the aerobic oxidation of HMF into DFF, in which the content of graphitic-N plays the determined role. What's more, the content of P-C species of the P-C-N-n-T catalysts favors the selectivity of DFF.

As discussed above, the P-C-N-5-800 catalyst exhibits the best performance for the conversion of HMF to DFF which was thus fixed as the catalyst in the following experiments if not otherwise indicated.

Table 3. Oxidation HMF into DFF with different P-C-N-5-T carbon catalysts synthesized by different annealing temperature

Entry	catalyst	HMF Con. (%)	DFF yield (%)	DFF Sel. (%)
1	P-C-N-5-600	61.9	37.5	60.6
2	P-C-N-5-700	82.3	73.6	89.4
3	P-C-N-5-800	93.6	93.6	100.0
4	P-C-N-5-900	57.0	56.4	99.5

Reaction conditions: HMF 1 mmol, catalyst 80 mg, 120 °C, MeCN 20 g, O_2 10 bar, 8 h.

Effect of solvents on the catalytic aerobic oxidation of HMF to DFF

The catalytic activity of the P-C-N-5-800 catalyst was further investigated in different solvents, including MeCN, DMSO, dimethylformamide (DMF), dioxane, N-methyl-2-pyrrolidone (NMP) and ethanol, while the other reaction conditions were kept the same. The HMF conversion and the DFF selectivity in the different reaction solvents over the P-C-N-5-800 catalyst at 120 °C are shown in Table 4. It is interesting to note that similar HMF conversion and DFF selectivity over the P-C-N-5-800 catalyst were obtained using the polar aprotic solvents DMF (81.1%, 91.4%), DMSO (80.9%, 94.7%) and NMP (82.7%, 89.5%). Among all organic reaction systems, the reaction conducted in ethanol gave the lowest DFF yield, with the HMF conversion and DFF selectivity being 91.9% and 64.8%, respectively. A 94.3% HMF conversion and a 39.1% DFF selectivity were achieved using water as the reaction solvent. The highest HMF conversion (93.6%) and DFF selectivity (100%) over the P-C-N-5-800 carbon catalyst was achieved with MeCN and was therefore chosen as the reaction solvent system in the further investigations.

Previous studies have shown that the reaction solvent can have a great influence on the catalytic activity.[52-53] This may be attributed to the different properties of solvents, including polarity.[54]. Generally, compare with strong polarity solvents, such as DMSO, DMF, NMP, moderate polarity solvents usually offer a high DFF yield because of the higher solubility of HMF in these moderate polarity solvents. What is more, oxygen as one kind of non-polar material is more easily dissolved in these moderate polarity solvents. Although the reaction in ethanol give a high HMF conversion, but the selectivity of DFF is extremely lower than the reaction in other organic solvents. This can be ascribed to the formation of ether between HMF and ethanol. Thus, it is concluded that the MeCN is the best solvent for this reaction system.

Table 4. Catalytic performance of P-C-N-5-800 under different reaction solvent systems

Entry	solvent	HMF Con. (%)	DFF yield (%)	DFF Sel. (%)
1	MeCN	96.7	96.7	100
2	DMSO	80.9	76.6	94.7
3	DMF	81.1	74.1	91.4
4	Ethanol	91.9	59.6	64.8
5	NMP	82.7	74.0	89.5
6	1,4-Dioxane	79.3	63.6	80.2
7	water	94.3	36.8	39.1

Reaction conditions: HMF 1 mmol, catalyst 80 mg, solvent 20 g, 120 °C, O_2 10 bar, 8 h.

Effect of catalyst loading on the catalytic aerobic oxidation of HMF to DFF

The effect of catalyst loading on the selective aerobic oxidation of HMF to DFF was also evaluated over P-C-N-5-800 catalyst under the given reaction condition, as shown in Figure 8. The catalyst loading has a significant effect on HMF conversion and thus DFF yield. When the amount of the catalyst was increased from 20 mg to 80 mg, the conversion of HMF rapidly increased from 15.6% to 93.6%. The results indicate that the conversion of HMF is positively related to the catalyst loading, with a nearly linear correlation between the conversion of HMF and the loading of catalyst before 60 mg. This could be attributed to the fact that the active sites of the catalyst are proportional to the amount of catalyst added. While further increasing the catalyst amount to 100 mg, an up to 98.7% DFF yield was obtained, and HMF was almost completely converted. When the catalyst loading was more than 60 mg, an up to 100% selectivity of DFF was achieved, suggesting the disappearance of other side products. Based on the above results, the amount of P-C-N-5-800 catalyst was maintained at 80 mg for the further studies.

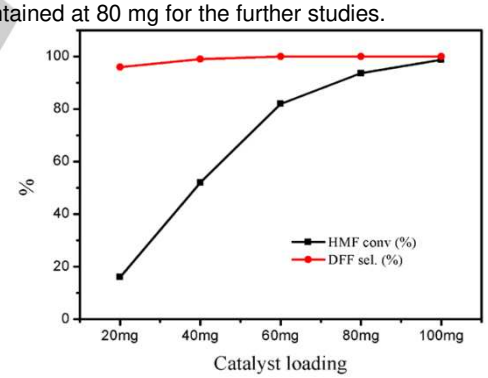

Figure 8. Effect of the P-C-N-5-800 catalyst loading on selectivity oxidation HMF to DFF. Reaction conditions: HMF 1 mmol, MeCN 20 g, O_2 10 bar, 120 °C, 8 h.

Effect of reaction temperature on the catalytic aerobic oxidation of HMF to DFF

The effect of reaction temperature (80-130 °C) on selective oxidation of HMF to DFF was also studied using the P-C-N-5-800 catalyst, while keeping the other reaction parameters constant. The results are depicted in Figure 9. HMF conversion is positively related to the reaction temperature while the selectivity to DFF is kept constantly high. When the reaction was conducted at 80 °C, the P-C-N-5-800 catalyst gave a poor catalytic activity, with the conversion of HMF and selectivity of DFF being 21.2% and 100% respectively. When the reaction temperature was increased from

80 °C to 120 °C, the conversion of HMF increased gradually from 21.2% (80 °C) to 93.6% (120 °C) while the selectivity to DFF was 100%. With further increase in the reaction temperature to 130 °C, a completely conversion of HMF was obtained. However, at this reaction temperature, HMF was found to start decomposing, forming other side products. Therefore, the optimum reaction temperature for this reaction over P-C-N-5-800 catalyst was determined to be 120 °C used hereafter.

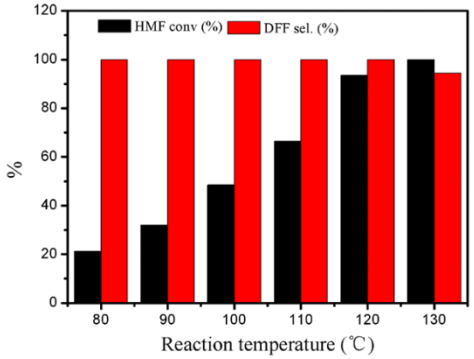

Figure 9. Effect of reaction temperature on the aerobic oxidation of HMF to DFF over the P-C-N-5-800 catalyst. Reaction conditions: HMF 1 mmol, catalyst 80 mg, MeCN 20 g, O_2 10 bar, 8 h.

Effect of oxygen pressure on the catalytic aerobic oxidation of HMF to DFF

The performance of P-C-N-5-800 catalyst for the catalytic aerobic oxidation of HMF to DFF was also examined at different oxygen pressure level at 120 °C for 8 h, and the results are presented in Figure 10. The pressure of oxygen was varied in the range of 2-10 bar. It was observed that the selectivity to DFF kept at nearly 100% while the conversion of HMF was sharply improved with an increase in oxygen pressure up to 6 bar. This is mainly due to the higher concentration of O_2 in the reactive solution under higher oxygen pressure. Above 6 bar, there was no obvious increase in DFF formation and HMF conversion.

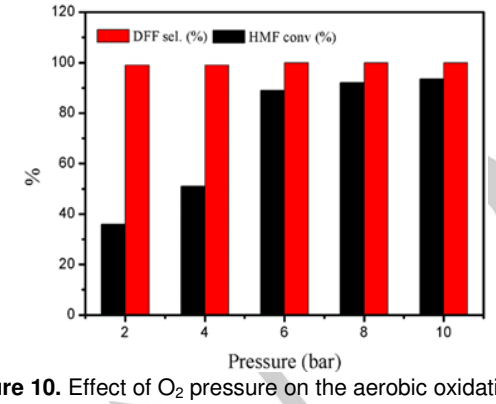

Figure 10. Effect of O_2 pressure on the aerobic oxidation of HMF to DFF over the P-C-N-5-800 catalyst. Reaction conditions: HMF 1 mmol, catalyst 80 mg, MeCN 20 g, 120 °C, 8 h.

Effect of reaction time on the catalytic aerobic oxidation of HMF to DFF

The effect of reaction time on the aerobic oxidation of HMF to DFF at 120 °C over the P-C-N-5-800 carbon catalyst was also investigated and the results are shown in Figure 11. The result suggests that the effect of reaction time on the selectivity of DFF is negligible while the HMF conversion and DFF yield were positively related to the reaction time. Both the conversion of HMF and the yield of DFF increased almost linearly with time. When the reaction time increased to 9 h, HMF was almost completely converted with a 99.5% yield of DFF. Notably, nearly 100% DFF selectivity was obtained at all tested times, implying that DFF is very stable under the given reaction conditions.

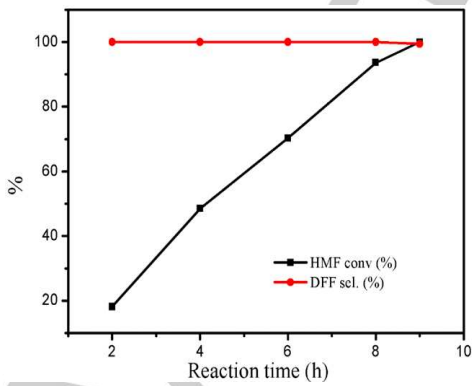

Figure 11. The time course of HMF oxidation into DFF over the P-C-N-5-800 catalyst. Reaction conditions: HMF 1 mmol, catalyst 80 mg,120 °C, MeCN 20 g, O_2 10 bar.

Reusability of P-C-N-5-800 catalyst

The final and important factor studied was the stability of the current catalyst. In order to investigate the stability and reusability of P-C-N-5-800 catalyst for the selective aerobic oxidation of HMF to DFF, six consecutive oxidation experiments were performed under the same reaction conditions and the results are given in Figure 12. After each run, the catalyst was recovered by filtration, washed with 75% ethanol and dried at 80 °C for 12h. Each reuse was scaled down to avoid the impact of catalyst loss. It was surprising that there was no evidence of any detectable decrease in catalyst activity even after six rounds of reuse, demonstrating a highly stable and easily recoverable material under the reaction conditions.

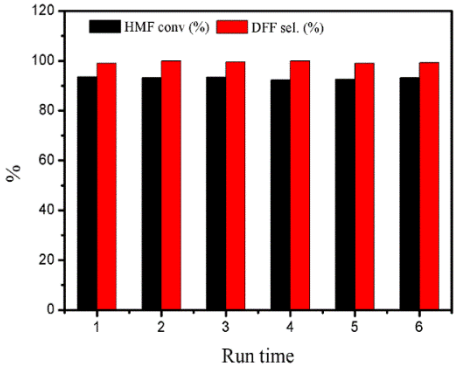

Figure 12. P-C-N-5-800 catalyst recyclability study in the oxidation of HMF to DFF. Reaction conditions: 120 °C, O_2 10 bar, MeCN 20g, 8h.

Conclusion

A series of metal-free carbon materials co-doped with P and N heteroatoms with high surface area have been successfully prepared and used for the selective aerobic oxidation of HMF to DFF. P-C-N-5-800, obtained with the optimized annealing temperature of 800 °C and mass ratio of phytic acid/C_3N_4 of 5,

possessed unprecedented activity and selectivity in the catalytic aerobic oxidation of HMF to DFF, giving a 99.5% DFF yield at 120 °C for 9 h under 10 bar oxygen pressure, the highest ever reported. Reusability studies further reveal that the P-C-N-5-800 catalyst is stable and re-usable without any evidence of deactivation. It is believed that this eco-friendly and robust metal-free catalyst might pave the way for large-scale production of DFF, as a biomass-derived industrial fuel and chemical.

Experimental Section

Materials

DFF (98%) and HMF (98%) were of analytical grade and purchased from Aladdin Chemicals Co., Ltd. (Shanghai, China). Urea and glucose were purchased from Sinopharm Chemical Reagent Co., Ltd. (Shanghai, China). Phytic acid solution 50 % (w/w) in H_2O was purchased from Tianjin Guangfu Chemical Industry (Tianjin, China). All other chemicals and solvents were purchased from Shanghai Titan Scientific Co., Ltd. (Shanghai, China) and they were analytically pure. All chemicals were used without further purification.

Catalyst preparation

Preparation of N doped carbon catalyst C_3N_4

The N doped carbon catalyst was prepared via a pyrolysis method. Briefly, a predetermined amount of urea was subjected to calcination at 550 °C for 4 h under an argon atmosphere with a heating rate of 3 °C/min. The obtained yellow powder was denoted as C_3N_4.

Preparation of P doped carbon catalyst P-C-800

P doped carbon catalyst was prepared as follows: the 50% phytic acid solution was evaporated firstly in an oven at 120 °C for 24 h, followed by being roasted at 800 °C for 4 h under an argon atmosphere with a heating rate of 3 °C/min. The obtained product was denoted as P-C-800 catalyst.

Preparation of P and N co-doped carbon catalysts P-C-N

The phytic acid solution as a phosphorus source was mixed with the as-prepared C_3N_4 and stirred finely and manually at room temperature. The mass ratio of phytic acid to C_3N_4 was varied by adjusting their relative ratios from 2.5:1 to 7.5:1. After that, the mixture was slowly evaporated at 120°C overnight in an oven. The obtained semi-solidified mixture was further calcined in a muffle furnace at different temperatures (600, 700, 800, 900 °C) for 4 h under an argon atmosphere with a heating rate of 3 °C /min. The obtained black powder was named as P-C-N-n-T, where the n and T represent the nmass ratio of phytic acid/C_3N_4 and the annealing temperature, respectively.

Catalyst characterization

Morphological characterization of the prepared carbon catalysts was carried out using a JSM-7500F scan electron microscope (SEM) instrument at an acceleration voltage of 20 kV. The microstructures of prepared samples were visualized on a JEOL JEM-2100 transmission electron microscope (TEM) instrument at an accelerating voltage of 200 kV. The TEM specimens were prepared by dissolving little of carbon catalysts powder in ethanol and dropping onto copper grids before measurement. X-ray diffraction (XRD) patterns of the synthesized samples were collected on a Bruker advanced D8 powder diffractometer in the 2θ range between 10-80° with Cu-kα radiation at a scanning rate of 0.016 ◦/s. Raman spectra were recorded on a Horiba Jobin Yvon LabRAM HR800 Raman spectrometer. The texture structures of the synthesized carbon catalysts were measured by N_2 adsorption-desorption using an ASAP2020 Micromeritics. The samples were outgassed at 350 °C for 4 h prior to the measurement. The specific surface areas and the pore size distributions were calculated using the Brunauer-Emmett-Teller (BET) method and the density functional theory (DFT) method respectively. The binding energies of the prepared carbon catalysts were collected on an X-ray photoelectron spectrometer (XPS, PHI-5702). All results of samples were corrected to the standard peak of C1s at 284.6 eV. Elemental mapping was carried out by using STEM-EDS.

Catalytic reaction

Catalytic performance measurements were carried out in a 70 ml Teflon-lined stainless steel autoclave equipped with an oil bath with a magnetic stirrer under high pressures. In a typical reaction, 1 mmol HMF, 20 g solvent, and 80 mg catalysts were successively added into the 70 ml Teflon-lined stainless-steel autoclave. After pre-purged with O_2 for 10 min, the reactor was filled with O_2 to a target pressure at room temperature. The reactor was then heated by hot oil with a stirring rate of 600 rpm by a magnetic stirrer. Once the system reached the desired temperature (e.g. 110 °C), the reaction was initiated. At the end of the reaction, the reactor bath was cooled to room temperature with ice water. The product was collected, separated using an oil phase filter, and analyzed by high performance liquid chromatography (HPLC) instrument equipped with an UV detector and a reversed phase C18 column.

Acknowledgements

This research did not receive any specific grant from funding agencies in the public, commercial, or not-for-profit sectors. The authors thank Research Center of Analysis and Test of East China University of Science and Technology for the help on the characterization.

Keywords: 5-hydroxymethylfurfural (HMF); 2,5-furandialdehyde (DFF); metal-free catalyst; oxidation

[1] J. Wang, J. Ren, X. Liu, J. Xi, Q. Xia, Y. Zu, G. Lu and Y. Wang, *Green Chem.* **2012**, *14*, 2506-2512.

[2] S. Fulignati, C. Antonetti, D. Licursi, M. Pieraccioni, E. Wilbers, H. J. Heeres and A. M. Raspolli Galletti, *Appl. Catal. A* **2019**,*578*, 122-133.

[3] B. S. Solanki and C. V. Rode, *Green Chem.* **2019**, 21, 6390-6406.

[4] P. V. Rathod and V. H. Jadhav, *ACS Sustainable Chem. Eng.* **2018**, *6*, 5766-5771.

[5] M. Kim, Y. Su, A. Fukuoka, E. J. M. Hensen and K. Nakajima, *Angew. Chem. Int. Ed.* **2018**, *57*, 8235-8239.

[6] B. Xiao, M. Zheng, X. Li, J. Pang, R. Sun, H. Wang, X. Pang, A. Wang, X. Wang and T. Zhang, *Green Chem.* **2016**, *18*, 2175-2184.

[7] B. Girisuta, L. P. B. M. Janssen and H. J. Heeres, *Green Chem.* **2006**, *8*, 701-709.

[8] Y. Mori, Y. Horikawa, T. Shikata and N. Kasuya, *J.Fiber.Sci.technol.* **2017**, *73*, 270-275.

[9] M. Hong, J. Min, S. Wu, H. Cui, Y. Zhao, J. Li and S. Wang, *ACS Omega.* **2019**, *4*, 7054-7060.

[10] P. V. Rathod, S. D. Nale and V. H. Jadhav, *ACS Sustainable Chem. Eng.* **2017**, *5*, 701-707.

[11] G. Yi, S. P. Teong and Y. Zhang, *Green Chem.* **2016**, *18,* 979-983.

[12] S. Xu, P. Zhou, Z. Zhang, C. Yang, B. Zhang, K. Deng, S. Bottle and H. Zhu, *J. Am. Chem. Soc.* **2017**, *139*, 14775-14782.

[13] M. Hong, J. Min, S. Wu, H. Cui, Y. Zhao, J. Li, S. Wang, *ACS Omega.* **2019**, *4*, 7054-7060.

[14] X. Liu, H. Ding, Q. Xu, W. Zhong, D. Yin, S. Su, *J. Energ. Chem.* **2016**, *25*, 117-121.

[15] C. Laugel, B. Estrine, J. Le Bras, N. Hoffmann, S. Marinkovic, J. Muzart, *ChemCatChem* **2014**, *6*, 1195-1198.
[16] M. Chatterjee, T. Ishizaka, A. Chatterjee and H. Kawanami, *Green Chem.* **2017**, *19*, 1315-1326.
[17] B. Ma, Y. Wang, X. Guo, X. Tong, C. Liu, Y. Wang and X. Guo, *Appl. Catal. A* **2018**, *552*, 70-76.
[18] L. Özcan, P. Yalçın, O. Alagöz and S. Yurdakal, *Catal. Today*. **2017**, *281*, 205-213.
[19] E. Hayashi, T. Komanoya, K. Kamata and M. Hara, *ChemSusChem* **2017**, *10*, 654-658.
[20] D. K. Mishra, H. J. Lee, J. Kim, H.-S. Lee, J. K. Cho, Y.-W. Suh, Y. Yi and Y. J. Kim, *Green Chem.* **2017**, *19*, 1619-1623.
[21] Z. L. Yuan, B. Liu, P. Zhou, Z. H. Zhang and Q. Chi, *Catal. Sci. Technol.* **2018**, *8*, 4430-4439.
[22] Y. Yan, K. Li, J. Zhao, W. Cai, Y. Yang and J.-M. Lee, *Appl. Catal. B* **2017**, *207*, 358-365.
[23] J. Zhao, X. Chen, Y. Du, Y. Yang and J.-M. Lee, *Appl. Catal. A* **2018**, *568*, 16-22.
[24] J. Lai, S. Zhou, F. Cheng, D. Guo, X. Liu, Q. Xu, D. Yin, *Catal. Lett.* **2020**,*150*, 1301-1308.
[25] X. Liu, J. Xiao, H. Ding, W. Zhong, Q. Xu, S. Su, D. Yin, *Chem. Eng. J.* **2016**, *283*, 1315-1321.
[26] S. Biswas, B. Dutta, A. Mannodi-Kanakkithodi, R. Clarke, W. Song, R. Ramprasad and S. L. Suib, *Chem. Commun.* **2017**, *53*, 11751-11754.
[27] Y. Ren, Z. Yuan, K. Lv, J. Sun, Z. Zhang and Q. Chi, *Green Chem.* **2018**, *20*, 4946-4956.
[28] Y. Sun, J. Jiang, Y. Liu, S. Wu and J. Zou, *Appl. Surf. Sci.* **2018**, *430*, 362-370.
[29] N. F. F. Moreira, M. J. Sampaio, A. R. Ribeiro, C. G. Silva, J. L. Faria and A. M. T. Silva, *Appl. Catal. B* **2019**, *248*, 184-192.
[30] Y. Wang, X. Wang and M. Antonietti, *Angew. Chem. Int. Ed.* **2012**, *51*, 68-89.
[31] I. Krivtsov, E. I. García-López, G. Marcì, L. Palmisano, Z. Amghouz, J. R. García, S. Ordóñez and E. Díaz, *Appl. Catal. B* **2017**, *204*, 430-439.
[32] L. Zhang and Z. Xia, *J. Phys. Chem. C* **2011**, *115*, 11170-11176.
[33] X. Lu, D. Wang, L. Ge, L. Xiao, H. Zhang, L. Liu, J. Zhang, M. An and P. Yang, *New J. Chem.* **2018**, *42*, 19665-19670.
[34] M. Li, L. Zhang, Q. Xu, J. Niu and Z. Xia, *J. Catal.* **2014**, *314*, 66-72.
[35] G. Murdachaew and K. Laasonen, *J. Phys. Chem. C* **2018**, *122*, 25882-25892.
[36] J. Long, X. Xie, J. Xu, Q. Gu, L. Chen and X. Wang, *ACS Catal.* **2012**, *2*, 622-631.
[37] Z. Zhou, K. Liu, C. Lai, L. Zhang, J. Li, H. Hou, D. H. Reneker and H. Fong, *Polymer* **2010**, *51*, 2360-2367.
[38] A. C. Ferrari, *Phys. Rev. B* **2000**, 61, 14095-14107.
[39] S. Indrawirawan, H. Sun, X. Duan, S. Wang, *J. Mater. Chem. A* **2015**, *3*, 3432-3440.
[40] X. Hu, M. Fan, Y. Zhu, Q. Zhu, Q. Song, Z. Dong, *Green Chem.* **2019,** *21*, 5274-5283.
[41] K. Wang, P. Jiang, M. Yang, P. Ma, J. Qin, X. Huang, L. Ma, R. Li, *Green Chem.* **2019**, *21*, 2448-2461.
[42] J. Zhang, Z. Zhao, Z. Xia and L. Dai, *Nat. Nanotech.* **2015**, *10*, 444-452.
[43] B. Shi, Y. Su, L. Zhang, M. Huang, R. Liu and S. Zhao, *ACS Appl. Mater. Interfaces* **2016**, *8*, 10717-10725.
[44] A. Ananthanarayanan, Y. Wang, P. Routh, M. A. Sk, A. Than, M. Lin, J. Zhang, J. Chen, H. Sun and P. Chen, *Nanoscale.* **2015**, *7*, 8159-8165.
[45] J. Long, X. Xie, J. Xu, Q. Gu, L. Chen and X. Wang, *ACS Catal.* **2012**, *2*, 622-631.
[46] Z. Zhang, J. Sun, M. Dou, J. Ji and F. Wang, *ACS Appl. Mater. Interfaces* **2017**, *9*, 16236-16242.
[47] X. Mao, Z. Cao, Y. Yin, Z. Wang, H. Dong and S. Yang, *Int. J. Hydrogen Energy* **2018**, *43*, 10341-10350.
[48] Z.-W. Liu, F. Peng, H.-J. Wang, H. Yu, W.-X. Zheng and J. Yang, *Angew. Chem. Int. Ed.* **2011**, *50*, 3257-3261.
[49] S. Wang , E. Iyyamperumal , A. Roy, Y. Xue, D. Yu, L. Dai, *Angew. Chem. Int. Ed.* **2011**, *50*, 11756-11760.
[50] Y. Gao, G. Hu, J. Zhong, Z. Shi, Y, Zhu, D, Su, J, Wang, X. Bao, D. Ma, *Angew. Chem. Int. Ed.* **2013**, *52*, 2109−2113.
[51] M. A. Patel, F. Luo, M. R. Khoshi, E. Rabie, Q. Zhang, C. R. Flach, R. Mendelsohn, E. Garfunkel, M. Szostak, H. He, *ACS Nano* **2016**, *10*, 2305-2315
[52] Y. Guo and J. Chen, *ChemPlusChem* **2015**, *80*, 1760-1768.
[53] G. Lv, H. Wang, Y. Yang, X. Li, T. Deng, C. Chen, Y. Zhu and X. Hou, *Catal. Sci. Technol.* **2016**, *6*, 2377-2386.
[54] G. Lv, S. Chen, H. Zhu, M. Li and Y. Yang, *Appl. Surf. Sci.* **2018**, *458*, 24-31.

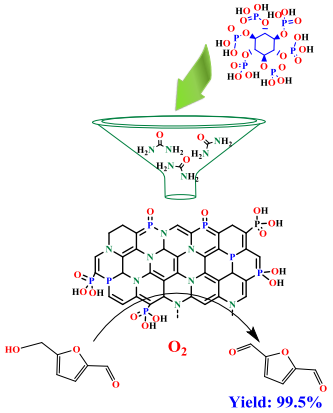

Phosphorus and nitrogen co-doped carbon (P-C-N) catalyst demonstrates a superb catalytic activity towards selective aerobic oxidation of 5-hydroxymethylfurfural (HMF) into 2,5-diformylfuran (DFF)